Inférence bayésienne pour l'estimation des propriétés thermophysiques des colonies de champignons filamenteux

Bayesian inference for the estimation of thermophysical properties of filamentous fungal colonies

Luiz Fernando Silva FERREIRA[1,2], Leonardo Antonio BERMEO VARON[3], Mayara Gil CASTRO SANTOS[5], Olivier FUDYM[1], Thomas PIERRE[4*,] Helcio R. B. ORLANDE[1]

[1]Federal University of Rio de Janeiro, COPPE/UFRJ, Rio de Janeiro, RJ, 21941-598, Brazil
[2]Federal Institute of Education, Science and Technology, Paracambi, RJ, 26600-000, Brazil
[3]School of Electrical and Electronics Engineering, Universidad del Valle, 100-00, Cali, Colombia.
[4]Univ. Bretagne Sud, UMR CNRS 6027, IRDL, F-56100, Lorient, France.
[5]Laboratory BAKTRON, Rio de Janeiro, RJ, 20921-003, Brazil.

[*]Corresponding author: thomas.pierre@univ-ubs.fr

Résumé – Ce travail présente la vérification d'une solution à un problème inverse lié à la détection thermique de champignons. L'objectif de ce problème inverse est l'estimation des propriétés thermiques d'une couche uniforme de champignon lors d'expériences de laboratoire contrôlées. Des mesures de température transitoires de la surface du champignon sont disponibles pour la résolution du problème inverse obtenue par l'algorithme de Metropolis-Hastings avec un échantillonnage par deux blocs deparamètres. Des mesures simulées sont utilisées pour la vérification de la solution.

Abstract – This works presents the verification of an inverse problem solution related to the thermal detection of fungi. The objective of the inverse problem is the estimation of the thermal properties of a uniform layer of a fungus in controlled laboratory experiments. Transient temperature measurements of the surface of the fungus are available for the inverse problem solution, which is obtained by using the Metropolis-Hastings algorithm with sampling by two blocks of parameters. Simulated measurements are used for the inverse problem solution verification.

Nomenclature

<u>Latine letters</u>

C	volumetric heat capacity, $J \cdot m^{-3} \cdot K^{-1}$
c	Specific heat, $J \cdot kg^{-1} \cdot K^{-1}$
h	heat transfer coefficient, $W \cdot m^{-2} \cdot K^{-1}$
k	thermal conductivity, $W \cdot m^{-1} \cdot K^{-1}$
L	length, m
$\mathbf{P}$	vector of model parameters
$\boldsymbol{k}$	unit vector
T	temperature, K
t	time, s
$\mathbf{V}$	covariance matrix
x	spatial coordinate, m
$\mathbf{Y}$	vector of measured temperatures, °C

<u>Greek letters</u>

μ	mean of prior distributions
ρ	density, $kg \cdot m^{-3}$
σ	standard deviation of measurement errors, °C

<u>Indices and exponents</u>

a	agar gel
f	*fungus*
ini	initial condition
p	plastic
∞	ambient/surroundings

https://doi.org/10.25855/SFT2026-043

1. Introduction

Several toxigenic fungi can result in significant risks to humans, animals and industrialized products [1, 2]. Grains, leaves, fruits, and other dairy products can be affected by mycotoxins produced by such fungi colonies [3]. Although JECFA [4] and ANVISA [5, 6] have established intake thresholds of such microorganisms, clinical detection of intoxication is complicated by biotransformation and a lack of literature correlating exposure to specific disease states [2]. Therefore, the early detection and control of fungi can contribute to diminish health problems [7]. This work aims to detect the presence of fungi from infrared images processing. To this end, the knowledge of thermophysical properties is necessary.

This work follows our previous studies involving the estimation of the thermophysical properties of a fungus or of fungi colonies in controlled laboratory experiments. These studies were based on different mathematical models depending on the situation under analysis, such as a lumped formulation for small fungal colonies [8] and one-dimensional heat conduction through uniform layers [9, 10]. The inverse analyses in these studies were all performed using the Markov Chain Monte Carlo (MCMC) method implemented through the Metropolis-Hastings algorithm [11–17].

Unlike standard studies that relied on the metabolic heat generation from active colonies for the thermal contrast [3, 18], our works considered transient cooling processes for the estimation of fungi thermal properties. In our previous works [9, 10], the sample was actively heated by a Flash pulse at the beginning of the experiment, which unfortunately did not result in consistent estimates when different regions of the fungus were used for the measurements. Here, we consider that the sample containing a uniform layer of fungus grown over agar gel in a Petri dish is initially in thermal equilibrium inside a biological incubator. The sample is removed from the incubator and naturally cooled to the surrounding environment. During the cooling period, temperature measurements are supposedly taken with an infrared camera of the surface of the fugus open to the surrounding environment. These measurements are then used in the inverse analysis, that is aimed at the estimation of the thermal properties of the fungus. Depending on the inoculation process in a Petri dish containing agar gel, a uniform layer of fungus can be formed, as presented by Figure 1, which shows one of our experiments with a Petri dish inoculated with *Aspergillus brasiliensis* [19–21].

The advantage of the approach is to observe, with contactless measurements, the thermal relaxation of a sample previously in equilibrium within a controlled thermal chamber, which is particularly well suited to the characterization of micro-organisms in culture media and avoids disturbing the medium with a more or less intense thermal excitation.

One difficulty with biological media is the presence of moisture transfer, but this phenomenon is neglected herein. However, observing a simple thermal relaxation in the absence of thermal excitation helps to mitigate their effects.

Figure 1: *Petri dish inoculated with* Aspergillus brasiliensis.

2. Methodology

2.1. Physical Problem and Mathematical Formulation

The physical problem involves one-dimensional heat conduction in a medium with three layers, corresponding to the fungus, agar gel and plastic (material of the Petri dish wall), with thicknesses L_f, L_a and L_p, respectively (see Figure 2). The layers are in perfect thermal contact, so that the heat conduction equation for this composite domain is given by:

$$C(x)\frac{\partial T(x,t)}{\partial t} = \frac{\partial}{\partial x}\left[k(x) \quad \frac{\partial T(x,t)}{\partial x}\right] \qquad , 0 < x < (L_f + L_a + L_p) \, , t > 0 \tag{1a}$$

where $C(x) = \rho(x)c(x)$ is the volumetric heat capacity, $k(x)$ is the thermal conductivity. Heat transfer through the boundary at $x = (L_f + L_a + L_p)$ is neglected, since the sample is supposed to be located over a thermal insulating material. The sample is cooled by convection and radiation through the boundary at $x = 0$, where T_∞ is the temperature of the surroundings and h is the combined convection and linearized radiation heat transfer coefficient. The initial temperature of the medium is uniform and given by T_{ini}. Therefore, boundary and initial conditions are given by:

$$-k_1\frac{\partial T(x,t)}{\partial x} + hT(x,t) = hT_\infty, \quad x = 0, \quad t > 0 \tag{1b}$$

$$k_p\frac{\partial T}{\partial x} = 0, \quad x = L_f + L_a + L_p, \quad t > 0 \tag{1c}$$

$$T(x,t) = T_{ini}, \quad 0 < x < L_f + L_a + L_p, \quad t = 0 \tag{1d}$$

Figure 2: *One-dimensional domain with three layers.*

2.2. Inverse Problem

The inverse problem of interest for this work is focused on the estimation of the volumetric heat capacity and thermal conductivity of the fungus layer, by using transient measurements taken at the surface $x = 0$. The inverse problem is solved within the Bayesian framework of statistics, where prior information available for all model parameters is taken into account [12-18]. The vector of model parameters is given by:

$$\boldsymbol{P}^T = [\boldsymbol{P}_1^T, \ \boldsymbol{P}_2^T] \tag{2a}$$

$$\boldsymbol{P}_1^T = \left[L_p, k_a, k_p, C_a, C_p, T_\infty, T_{ini}\right] \tag{2b}$$

$$\boldsymbol{P}_2^T = \left[L_a, L_f, C_f, k_f, h\right] \tag{2c}$$

and the subscripts *f, a* and *p* refer to the fungus, agar gel and Petri dish wall, respectively.

The vector $\boldsymbol{P}_1$contains the parameters for which quite informative priors are available, while the vector $\boldsymbol{P}_2$ includes the parameters that are *a priori* known with larger uncertainties. Priors for all model parameters were considered as independent truncated Gaussian distributions, with means $\boldsymbol{\mu}_1$ and $\boldsymbol{\mu}_2$, and covariance matrices $\boldsymbol{V}_1$ and $\boldsymbol{V}_2$, for $\boldsymbol{P}_1$and $\boldsymbol{P}_2$, respectively. Measurement errors, **Y**, were assumed as additive, Gaussian, with zero mean, uncorrelated and with constant standard deviation σ. Therefore, the posterior distribution is given by:

$$p(\boldsymbol{P}|\boldsymbol{Y}) \propto exp\left\{-\frac{1}{2}\frac{[\boldsymbol{Y}-\boldsymbol{T}(\boldsymbol{P})]^T[\boldsymbol{Y}-\boldsymbol{T}(\boldsymbol{P})]}{\sigma^2}\dots \right.$$
$$\left. -\frac{1}{2}(\boldsymbol{P}_1-\boldsymbol{\mu}_1)^T\boldsymbol{V}_1^{-1}(\boldsymbol{P}_1-\boldsymbol{\mu}_1)-\frac{1}{2}(\boldsymbol{P}_2-\boldsymbol{\mu}_2)^T\boldsymbol{V}_2^{-1}(\boldsymbol{P}_2-\boldsymbol{\mu}_2)\right\} \quad (3)$$

for $\boldsymbol{P}_{1,min} \le \boldsymbol{P}_1 \le \boldsymbol{P}_{1,max}$ and $\boldsymbol{P}_{2,min} \le \boldsymbol{P}_2 \le \boldsymbol{P}_{2,max}$, with $p(\boldsymbol{P}|\boldsymbol{Y}) = 0$ elsewhere, where $\boldsymbol{T}(\boldsymbol{P})$ is the solution of the direct problem given by eqs. (1a-d) with known parameters **P**.

Samples of the posterior distribution for **P** were generated in this work by using the Metropolis-Hastings algorithm with sequential sampling by two blocks of parameters[12, 17].

3. Results

The direct problem given by eq. (1a-c) was solved with implicit finite-volumes, by using 60 volumes and a time-step of 10 s. The direct problem solution was verified by solving the same problem with COMSOL, with 101 finite-elements and a time-step of 0.01 s. The exact value of the $\mathbf{P_2}$ block used for the simulation were respectively: L_a = 1.5 mm; L_f = 1.5 mm; $C_f = 0.836 \times 10^6$ J·m^{-3}·K^{-1}; $k_f = 1.66$ W·m^{-1}·K^{-1}; $h = 35$ W·m^{-2}·K^{-1}

Figure 3 presents a comparison of these two solutions at x = 0, which exhibit a perfect agreement on the graph scale. In order to avoid an inverse crime, the simulated measurements were generated with the COMSOL solution, by adding a Gaussian random noise with standard deviation of 0.5 °C. The simulated measurements are illustrated in Figure 4. The measurements were supposed available with a frequency of 0.1 Hz, and the experimental data was used for the solution of the inverse problem until the final time of 1 200 s.

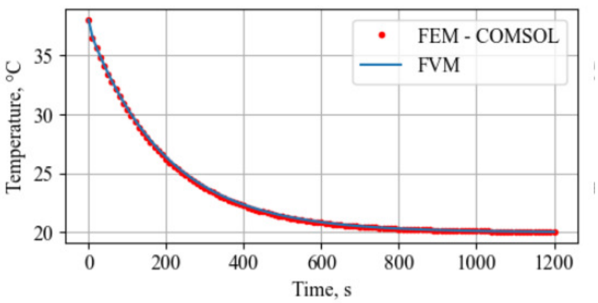

Figure 3: *Verification of the direct problem solution.*

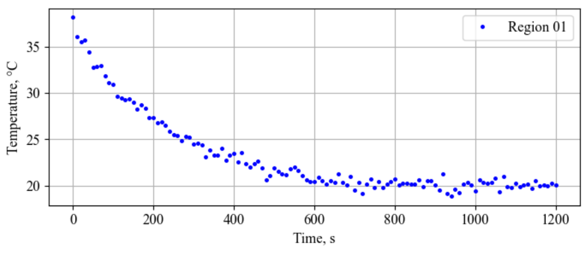

Figure 4: *Simulated Measurements.*

The values of means, standard-deviations, minima and maxima for the truncated Gaussian priors used in this work are presented in Table 1. The Markov chains were simulated with 10^5 samples, and statistics of the posterior were calculated by discarding the first 10^4 samples (burn in period). Candidate samples for $\boldsymbol{P}_1$were generated from their priors, while a random walk process obtained from a uniform distribution was used to generate candidates for $\boldsymbol{P}_2$. The resulting acceptance rate was 28 %. The Markov chains were started at 10% above the respective mean values for $\boldsymbol{P}_1$ parameters and 20 % above the respective mean values for $\boldsymbol{P}_2$ parameters.

Parameter	*Mean*	Std. Dev.	Min.	Max.
L_p, mm	0.8	0.008	0.008	80.0
k_a, W·m^{-1}·K^{-1}	1.2656	0.0127	0.0127	126.56
k_p, W·m^{-1}·K^{-1}	0.1603	0.0016	0.0016	16.03
C_a, J·m^{-3}·K^{-1}	1.968×10^6	1.968×10^4	1.97×10^4	1.97×10^8
C_p, J·m^{-3}·K^{-1}	1.521×10^6	1.521×10^4	1.52×10^4	1.52×10^8
T_∞, °C	20.0	0.20	0.20	2000.0
T_{ini} , °C	38.0	0.38	0.38	3800.0
L_a, mm	1.5	0.15	0.15	5.0
L_f, mm	2.5	0.25	0.15	3.0
C_f, J·m^{-3}·K^{-1}	1.968×10^6	7.0×10^5	1.0×10^5	6.0×10^6
k_f W·m^{-1}·K^{-1}	2.20	0.60	0.01	132.9
h, W·m^{-2}·K^{-1}	35.0	2.0	20.0	100

Table 1: *Truncated Gaussian priors for* $\boldsymbol{P}_1$ *and* $\boldsymbol{P}_2$*.*

The Markov chains, as well as the histograms of the samples after the burn-in period, are presented in Figures 5a,b, for C_f and k_f, respectively. An analysis of these figures reveals that the Markov chains reached convergence for both parameters, with means very close to the exact values of the parameters that were used to generate the simulated measurements. In fact, Figure 6 presents Geweke's analysis for convergence of the Markov chains [12, 17] for parameters $\boldsymbol{P}_2$, thus demonstrating that the means at the beginning and end of the Markov chains differ by less than 2 %.

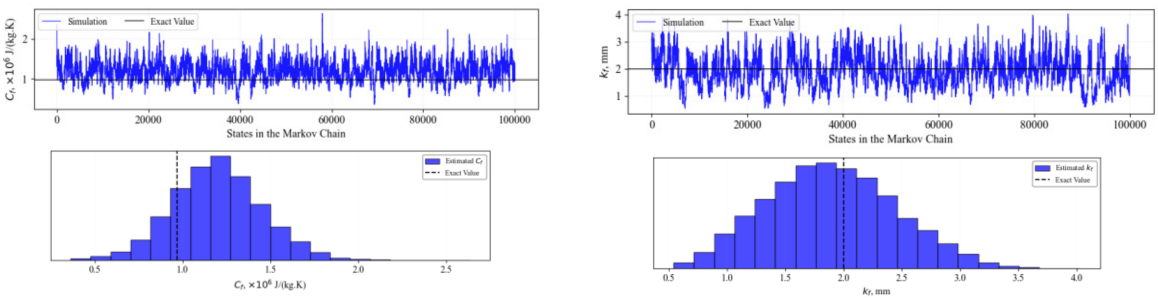

(a) (b)

Figure 5: *Markov Chains and histograms of: (a) C_f, and (b) k_f.*

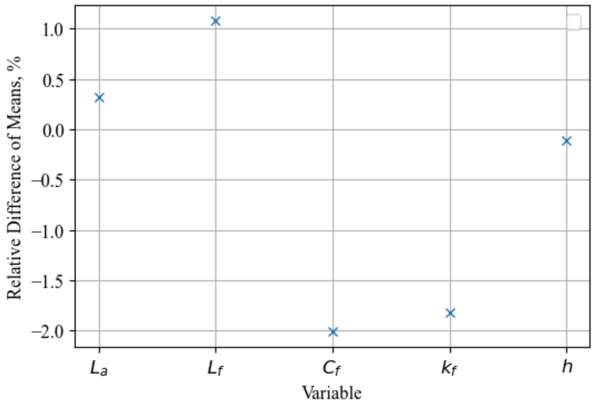

Figure 6: *Relative difference of means at the start of burn-in and end of the Markov chains.*

An important feature of the Markov Chain Monte Carlo (MCMC) method is that it naturally allows the simulation under uncertainty of the dependent variables of the direct problem, with the samples of the parameters at each state of the Markov chains. Figure 7 shows the temperature variation at the surface $x = 0$, estimated with the means of the parameters after the convergence of the Markov chains and the simulated measurements. The shadow area shown in this figure gives the 95 % credible interval of the estimated temperatures. Estimated temperatures follow very closely the measurements, as well as the exact temperatures shown in Figure 3.

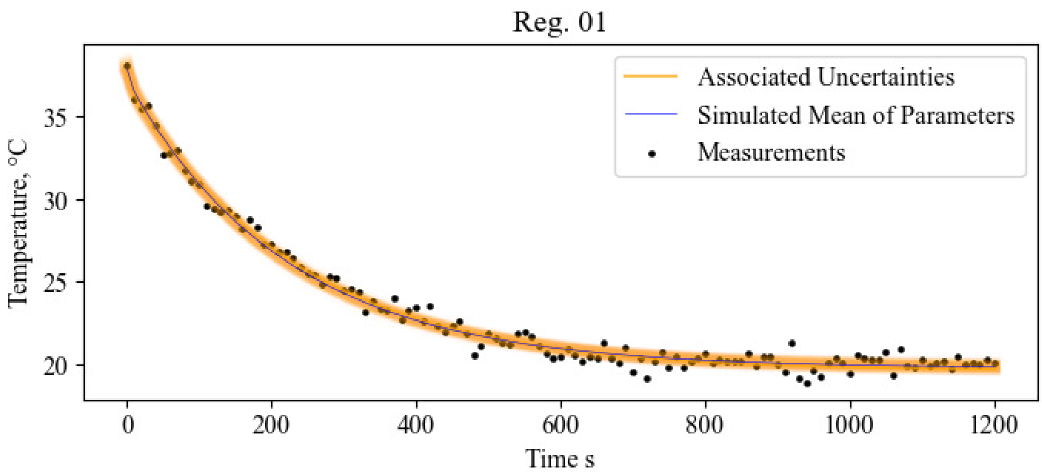

Figure 7: *Simulation under uncertainty of the temperature at x = 0.*

Statistics of the marginal posterior distributions of the parameters $\boldsymbol{P}_2$ are shown by Table 2, including the means, standard deviations and 2.5 % and 97.5 % percentiles of the samples of the equilibrium Markov Chains. This table shows significant reduction in standard deviation only for C_f, while the other parameters kept similar values for their statistics despite they reduced the range of the credible interval.

Parameter	*Mean*	*Standard dev.*	*95 % C. I.*
L_a, mm	1.558	0.159	(1.16, 1.9)
L_f, mm	2.576	0.259	(1.95, 3.2)
C_f, J·m^{-3}·K^{-1}	0.836×10^6	2.33×10^5	$(0.68 \times 10^6, 2.04 \times 10^6)$
k_f,W·m^{-1}·K^{-1}	1.66	0.604	(0.483, 3.282)
h, W·m^{-2}·K^{-1}	35.02	2.08	(30.21, 40.20)

Table 2: *Statistics of the posterior distributions for* $\boldsymbol{P}_2$.

4. Conclusions

This work presented the verification of an inverse problem solution aimed at the estimation of the thermophysical properties of a uniform layer of filamentous fungus. The inverse analysis was performed within the Bayesian framework of statistics, by using the Metropolis-Hastings algorithm with sequential sampling by blocks of parameters, which allowed for the simultaneous estimation of the parameters and their associated uncertainties. The results obtained with simulated measurements, containing additive Gaussian noise to mimic experimental conditions, demonstrated the effectiveness of the proposed methodology. The Markov chains for the parameters of interest exhibited satisfactory convergence, and the estimated values showed excellent agreement with the exact values used for the simulation. Therefore, this study confirms the feasibility of the computational approach for characterizing the thermal properties of biological samples. These findings support the application of this methodology to experimental data obtained from real fungal colonies, an investigation that is currently in progress.

References

[1] M. T. Maziero, L. D. S. Bersot, Micotoxinas em alimentos produzidos no Brasil, *Rev. Bras. Prod. Agroind.*, 12 (2010) 89-99.

[2] G. D. Savi, F. S. Zenaide, Mycotoxins: risks to human health due to daily ingestion of contaminated food and its occurrence in clinical samples, *Res. Soc. Dev.*, 9 (2020) e24942482.

[3] K. Neme, A. Mohammed, Mycotoxin occurrence in grains and the role of postharvest management as a mitigation strategies. A review, *Food Control*, 78 (2017) 412-425.

[4] JECFA, WHO, *Safety evaluation of certain mycotoxins in food*, Food & Agriculture Org. (2001).

[5] ANVISA, *Resolução RDC n ° 7, de 18 de fevereiro de 2011*, Diário Oficial da União, Seção 1 (2011) 72.

[6] ANVISA, *Resolução RDC no 138, de 08 de fevereiro de 2017*, Diário Oficial da União, Seção 1 (2017).

[7] M. Frac, S. Jezierska-Tys, T. Yaguchi, Occurrence, Detection, and Molecular and Metabolic Characterization of Heat-Resistant Fungi in Soils and Plants and Their Risk to Human Health, *Adv. Agron.*, 132 (2015) 161–204.

[8] L. F. S. Ferreira, T. Pierre, L. A. B. Varon, H. R. B. Orlande, Thermal parameter estimation of mold in petri dishes by application of flashlight and thermal camera measurements, *Proc. Congrès Français de Thermique* (Reims, 30 mai-02 juin 2023), p. 024.

[9] L. F. S. Ferreira, H. R. B. Orlande, T. Pierre, L. A. B. Varon, Parameter Estimation Problem for the Thermal Characterization of a Fungus, *Proc. 11th Int. Conf. Inv. Prob. Eng.* (Búzios, 23-28 june 2024), 626-635.

[10] L. F. S. Ferreira, L. A. B. Varon, T. Pierre, M. G. C. Santos, O. Fudym, H. R. B. Orlande, Estimation of Thermophysical Properties of Filamentous Fungal Colonies, *Proc. 28th Int. Cong. Mech. Eng.* (Curitiba, 2025).

[11] D. Calvetti, E. Somersalo, *Introduction to Bayesian Scientific Computing*, Springer (2007).

[12] Gamerman, H. F. Lopes, *Markov Chain Monte Carlo: Stochastic Simulation for Bayesian Inference*, CRC Press (2006).
[13] C. J. Geyer, Introduction to Markov Chain Monte Carlo, in *Handbook of Markov Chain Monte Carlo*, CRC Press (2011) 3-48.
[14] J. P. Kaipio, C. Fox, The Bayesian framework for inverse problems in heat transfer, *Heat Transf. Eng*., 32 (2011) 718-753.
[15] J. P. Kaipio, E. Somersalo, *Statistical and Computational Inverse Problems*, Springer (2005).
[16] P. M. Lee, *Bayesian Statistics: An Introduction*, Wiley (2012).
[17] M. N. Özisik, H. R. B. Orlande, *Inverse Heat Transfer: Fundamentals and Applications*, CRC Press (2021).
[18] . Lipińska, K. Pobiega, K. Piwowarek, S. Błażejak, Research on the Use of Thermal Imaging as a Method for Detecting Fungal Growth in Apples, *Horticulturae*, 8-10 (2022) 972.
[19] L. Benoit, I. Malavazi, G. H. Goldman, S. E. Baker, R. P. de Vries, Aspergillus: Genomics of a Cosmopolitan Fungus, *The Mycota*, Springer (2013) 89-126.
[20] F. Ntana, U. H. Mortensen, C. Sarazin, R. Figge, Aspergillus: A Powerful Protein Production Platform, *Catalysts*, 10-9 (2020) 1064.
[21] A. Martirena-Ramirez, J. G. Serrano-Gamboa, Y. Pérez-Llano, C. O. Zenteno-Alegria, M. L. IzaArteaga, M. R. Sánchez-Carbente, A. M. Fernández-Ocaña, R. A. Batista-García, J. L. Folch-Mallol, Aspergillus brasiliensis E 15.1: A Novel Thermophilic Endophyte..., *J. Fungi*, 10 (2024) 517.

Acknowledgements

The financial support of FAPERJ and of the Embassy of France in Brazil for the visits of Thomas Pierre to UFRJ (2022) and of Helcio Orlande to IRDL-UBS (2024) is greatly appreciated. This work has also been supported by CNPq and CAPES. Leonardo Varón visited COPPE/UFRJ in 2020 within the CAPES-PRINT Program. The Ph.D. scholarship of Luiz Ferreira was provided by CNPq.